Module 5: Schlieren and Shadowgraph

Lecture 29: Review of optical techniques for imaging crystal growth

The Lecture Contains:

Previous Next

LASER MEASUREMENT TECHNIQUES AND DATA ANALYSIS

The optical configurations for interferometry, schlieren and shadowgraph as well as data retrieval from optical images are discussed in the following sections.

OPTICAL ARRANGEMENT

For measurements, a continuous wave helium-neon laser has been used as the coherent light source. A monochrome CCD camera (*Sony*, Model: XC-ST50) of spatial resolution of 768 X 574 pixels was used to record the convective field. The camera was interfaced with a personal computer (HCL, 256 MB RAM, 866 MHz) through an 8-bit A/D card. Interferograms, schlieren and shadowgraph images presented in this work have been subjected to image processing operations to improve contrast; the data analysis for recovering the field concentration and temperature are, however, based on the intensity changes in the original images.The layout for each of the three imaging techniques used in the present work is shown in Figure 5.15.

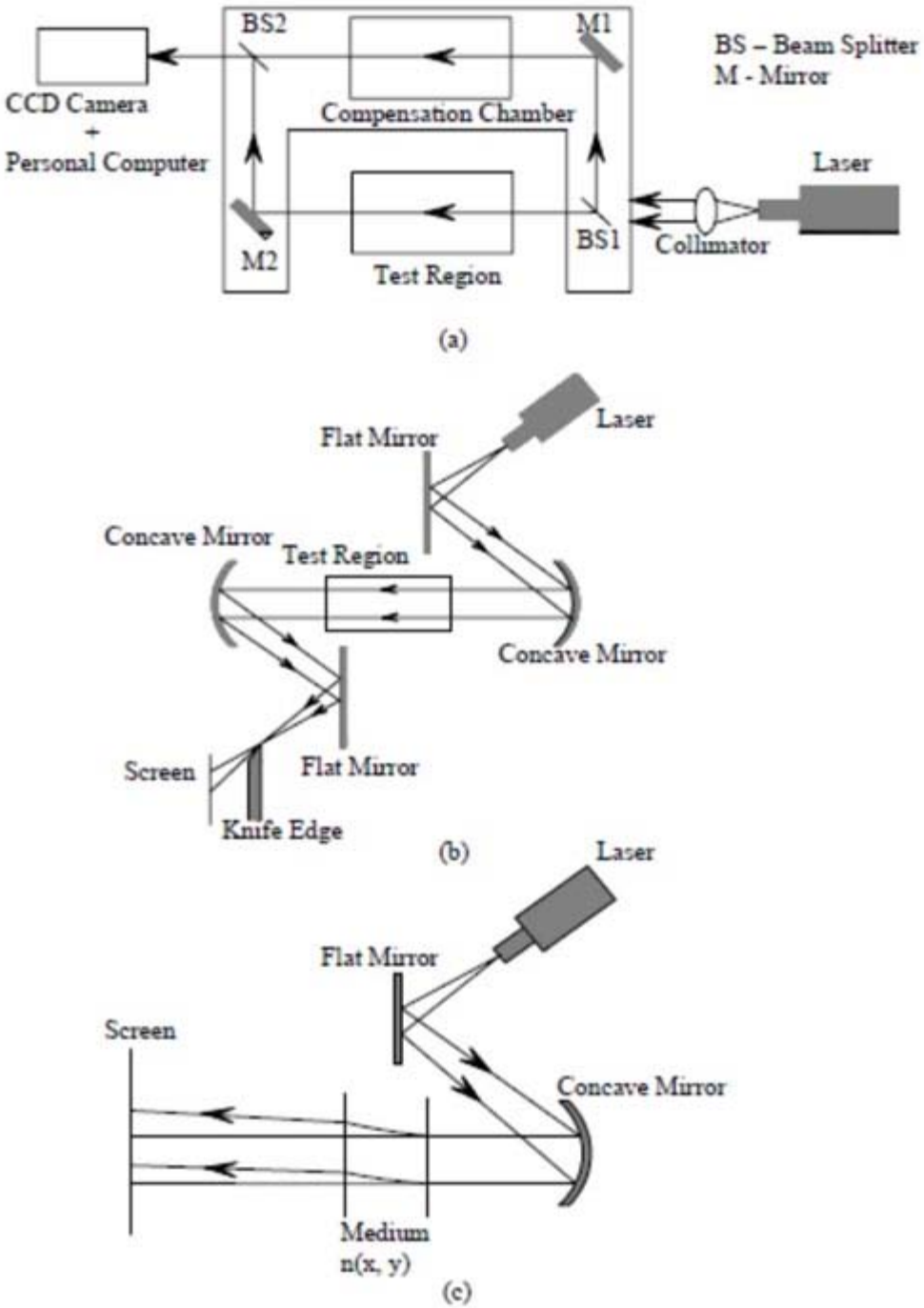

Figure 5.15: Optical layout of (a) Mach-Zender interferometer, (b) Schlieren and (c) Shadowgraph

The M-Z interferometer has two mirrors and two 50% beam splitters of 150 mm diameter. The mirrors are coated with 99.9% silver and employ a silicon dioxide layer as a protective layer. The interferometer floats on pneumatic legs to isolate the optics from external vibrations. Experiments have been carried out in the infinite as well as the wedge fringe setting. In the infinite fringe setting, the optical path difference between the test and the reference beams is initially zero. When a density disturbance is introduced in the path of the test beam, it is seen as a set of fringes over which the depth-averaged concentration or temprerature field is a constant. In the wedge fringe setting, the optics is slightly misaligned to produce a set of straight fringes. When exposed to a thermal or concentration field, the fringes are displaced to an extent depending on the change in temperature or concentration. The fringes in the wedge fringe setting of the interferometer are thus representative of

the temperature variation in the rectangular cavity and concentration profile in the crystal growth chamber. In the present work, the infinite fringe setting initially produced an image of uniform brightness indicating true constructive interference between the test and the reference beams. In the wedge fringe setting, the fringes were seen to be straight and horizontal.

Previous Next

The schlieren system used in the present work is of the ***Z***-type, as shown in Figure 5.15(b). The optics includes concave mirrors of 1.30 m focal length and 200 mm diameter. Relatively large focal lengths make the schlieren technique sensitive to the concentration gradients. The knife-edge is placed at the focal length of the second concave mirror. It is positioned to cut off a part of the light focused on it, so that in the absence of any optical disturbance, the illumination on the screen is uniformly reduced. The initial intensity values in the experiment were chosen to be less than 20, on a gray scale of 0-255. The knife-edge is set perpendicular to the direction in which the density gradients are to be recorded. In the present study, the gradients are expected to be predominantly in the vertical direction of gravity, and the knife-edge has been kept horizontal.

Shadowgraph images have been recorded using the same optical components as employed in the interferometry setup by first blocking the reference beam and allowing the test beam alone to fall on the screen. Shadowgraph images have also been recorded from the schlieren apparatus by collecting the refracted light beam emerging from the test cell (Figure 5.15(c)). The position of the screen on which the shadowgraph images are displayed plays an important role in data analysis. The screen position is chosen so as to improve the image contrast, while extracting the dominant features of the flow field. Beam refraction from regions of high concentration gradients can interfere with those passing through one of nearly constant concentration. This factor is taken into account while fixing the camera position. The initial intensity distribution in shadowgraph experiments corresponds to the Gaussian intensity variation of the laser source itself.

Previous Next

IMAGE PROCESSING

The three optical methods generate images that are path integrals of the refractive index fields and in turn, the concentration (or temperature) distribution in the fluid medium. The integrals can be simplified if the fields being studied are strictly two-dimensional. In general, the local information can be extracted using principles of tomography. In the present work, the images have been interpreted as carrying information of the solutal concentration (or temperature) field that is an average along the direction of propagation of light.

The determination of the concentration/temperature field from interferograms requires several intermediate steps, including (a) noise removal, (b) edge detection, (c) location of intensity minima within fringe bands, and (d) fringe thinning. Step (d) involves fitting a smooth function through points of intensity minima within a single fringe, as obtained in step (c). In addition, assigning temperatures to fringes, followed by transferring the data to a Cartesian grid are important. The fact that fringe thickness is small in regions of high concentration or temperature gradients has not been used in the present work. The analysis and interpretation of fringe patterns in interferometry has been discussed in detail by various authors. The approach described in has been implemented in the present study.

In contrast to interferometry where information is localized at the fringes, a schlieren image carries information related to the local temperature/concentration in the form of an intensity distribution. The advantage here is that data is available at the pixel-level of the camera. Drawbacks include the errors due to superimposed noise associated with scattering and the possibility of device saturation. In the present work, the first factor is taken to be less significant because the field variable is obtained by integrating the intensity distribution (see Data Reduction), an operation that tends to smooth noisy profiles. The second factor was circumvented by reducing the laser intensity using neutral density filters. The local temperatures (and concentrations) were then determined by numerically integrating the appropriate governing equation in the direction normal to the knife edge.

Previous Next

Data reduction

The present section examines the suitability of the three optical techniques of the present study for quantitative analysis of the convective field within a rectangular cavity and during crystal growth. An aspect shared by the three techniques is that they generate projection data, namely information that is integrated in the direction of propagation of the light beam. The result of analysis is thus a concentration (or temperature) that is ray-averaged over the length L of the growth chamber. The steps involved in the analysis of the experimental images are briefly discussed below.

Refractive index techniques depend on the fact that for a transparent material, refractive index and density share a unique relationship, called the Lorenz-Lorentz formula. In addition, if pressure changes within the fluid region are small, density will be uniquely related to solute concentration and temperature. The functionality is often linear since changes in concentration and temperature are often small in many applications. In rectangular cavity experiments, temperature is the only dependent variable and density (and hence refractive index) relates to temperature. Though crystal growth is driven by the cooling process of the solution, the ramp rate is often small enough for thermal equilibrium to prevail for short periods of time throughout the experiment. In the present analysis, it is assumed that the aqueous solution has negligible temperature gradients. Hence, refractive index becomes a measure of concentration itself. The material property that determines the sensitivity of the optical measurement is dn/dC where n is the refractive index and C is solute concentration.

Previous Next

The following discussion is presented in terms of solutal concentration. It is equally applicable to imaging thermal convection.

Interferometry

For a light source of wavelength λ the change in concentration required per fringe shift in the infinite fringe setting is given by the equation

$$\Delta C_s = \frac{\lambda / L}{dn/dC} \tag{1}$$

The fringe positions are to be determined from interferogram analysis. In the wedge fringe setting, it can be shown that the fringe displacement from the initial position is proportional to the change in concentration with respect to the portion of the solution where the fringes are undisturbed. These results hold under the approximation that refraction effects are small.

Schlieren

Image formation in a schlieren system is due to the deflection of light beam in a variable refractive index field towards regions that have a higher refractive index. In order to recover quantitative information from a schlieren image, one has to determine the cumulative angle of refraction of the light beam emerging from the growth chamber as a function of position in the $x-y$ plane. This plane is defined to be normal to the light beam, whose direction of propagation is along the $z-$coordinate. Using principles of ray-optics, the total angular deflection δ can be expressed as

$$\delta = \frac{1}{n_a} \int_0^L n \frac{\partial (\ln n)}{\partial y} \, dz$$

where n is the refractive index at any point in the solution. The change in the intensity field (ΔI) relative to the background (I_k) can now be related to the refractive index field directly as

$$\frac{\Delta I}{I_k} = \frac{f}{a_k \, n_a} \int_0^L \frac{\partial n}{\partial y} \, dz \tag{2}$$

Contd...

where $n_a(\sim 1)$ is the refractive index of the ambient, a_k is the size of the focal spot at the knife edge, and f is the focal length of the de-collimating mirror. This equation shows that the schlieren technique records the average gradient of refractive index over the path of the light beam. In terms of the ray-averaged refractive index, the governing equation for the schlieren process can be derived as:

$$\frac{\Delta I}{I_k} = \frac{f}{a_k}\frac{\partial n}{\partial l} L \qquad (3)$$

where L is the length of the path traversed by the light beam through the growth chamber, namely its diameter. Equation 3 requires the approximation that changes in the light intensity occur due to beam deflection, rather than its physical displacement. The concentration gradient is related with the refractive-index gradient of the KDP solution using the following relation

$$\frac{\partial N}{\partial y} = \frac{9n}{2\alpha\,(n^2+2)^2}\frac{\partial n}{\partial y} \qquad (4)$$

Here N is the molar concentration of the solution and *a* is the polarizability of the KDP crystal $(= 4.0\ cm^3/mole)$ Combining Equations 3 and 4 and integrating from a location in the bulk of the solution (where the gradients are negligible), the concentration distribution around the growing crystal can be uniquely determined.

The contribution of refraction of light at the confining optical windows has been accounted for by applying a correction factor in Equation 3 for the angle of deflection with which the beam emerges from the growth chamber. It can be shown using Snell's law that the correction factor is equal to the refractive index of the KDP solution (=1.355) at the ambient temperature.

Previous Next

Shadowgraph

The shadowgraph arrangement depends on the change in the light intensity arising from beam displacement from its original path. Shadowgraph analysis requires tracing the path of individual rays through the aqueous solution. When subjected to linear approximations that include small displacement of the light ray, a second order partial differential equation can be derived for the refractive index field with respect to the intensity contrast in the shadowgraph image. With Δ as the distance of the screen from the optical window on the beaker and D as the Laplace operator in the $x-y$ plane, this equation is

$$\frac{\Delta I}{I_k} = LD\left[\Delta\left\{\ln n\,(x,y)\right\}\right] \qquad (5)$$

Equations 2 and 5 have to be suitably integrated to determine the refractive index, and hence the concentration field. Integration of the Poisson equation (5) can be performed by a numerical technique, say the method of finite differences. When the approximations involved in Equations 2 and 5 do not apply, optical techniques can be used for flow visualization alone.

In interferometry, one can measure concentration values only at those points where fringes appear. The quantity of information is also limited by the number of fringes (infinite fringe setting) or their deformation (wedge fringe setting). Schlieren and shadowgraph generate information about the refractive index field at every pixel of the image in the form of intensities.

Previous Next

UNCERTAINTY AND MEASUREMENT ERRORS

Errors in the experimental data are associated with misalignment of the apparatus with respect to the light beam, noise generated at different stages of the experiment, including the imperfections of the optical components, and the intrinsic unsteadiness of the convection process itself. All experiments were conducted several times to establish the repeatability of the convective patterns, for the parameter range of interest. A quantitative assessment of errors and uncertainty was possible in experiments on convection in a rectangular cavity because of knowledge of the lower and upper surface temperatures.

A series of cross-checks have been enforced to validate the quantitative results obtained from experiments in the rectangular cavity. These include predicting the temperature of the cold top wall by starting from the lower hot wall, as well as comparing steady heat transfer rates across the cavity against published correlations. For example, an interferometry experiment with hot and cold temperatures of 305.5 K and 300.5 K yielded the cold wall temperature as 300.2 K. For temperatures of 300 and 320 K, the hot wall temperature was predicted to be 319.65 K. In schlieren, temperatures of 300 and 320 K were predicted as 301 and 319 K. The errors were considerably smaller at lower temperature differences across the cavity where the flow field was clearly steady. The comparison with correlations of average heat fluxes across the cavity for various temperature differences is discussed in Section Benchmark Experiment.

In experiments with air, the time-dependent movement of the fringes during interferometry and the time-wise change in intensity for schlieren were not severe enough at the lower end of temperature differences, specifically the lower end of the Rayleigh number range. For Ra>51,000 unsteadiness was a source of uncertainty in the local temperature profiles as well as the wall heat transfer rates. Quite often, unsteadiness was a source of measurement uncertainty in air. It was less serious in water as well as the aqueous solution of KDP. Analysis of convection patterns in the KDP solution could be carried out under conditions of mild unsteadiness by averaging a time-sequence of images. The results obtained in the present work can be taken to be quantitatively meaningful for the lower range of Rayleigh numbers. For very high Rayleigh numbers, the images are purely representative of the instantaneous thermal/solutal fields in the fluid region.

An additional check carried out in the crystal growth experiments was one of solutal mass balance. Since the convective field was imaged from various angles, it was possible to independently determine the average concentration of KDP on a given plane. These averages were within 0.1% of each other as long as the convection plume was steady. Larger discrepancies were seen in those experiments where the convection process was strongly unsteady. Only those images that satisfied the mass balance check were used for tomographic reconstruction.